Arabian Journal of Chemistry (2023) **16**, 105125

King Saud University

**Arabian Journal of Chemistry**

www.ksu.edu.sa
www.sciencedirect.com

ORIGINAL ARTICLE

# Sustainable and economical dolomite-modified biochar for efficient removal of anionic dyes

**Rabia Amen, Islam Elsayed, El Barbary Hassan** *

*Department of Sustainable Bioproducts, Mississippi State University, Box 9820 Mississippi State, MS 39762*

Received 1 May 2023; accepted 29 June 2023
Available online 4 July 2023

**KEYWORDS**

Biochar;
Dolomite;
Remazol brilliant blue;
Reactive black 5;
Water treatment

**Abstract** Dyes induce acute to chronic illnesses in humans and aquatic animals. This study tested dolomite-modified rice husk biochar (DRHB) to eliminate anionic reactive dyes Remazol Brilliant Blue (RBB) and Reactive Black 5 (RB-5) from simulated wastewater solutions. DRHB was produced by pretreating rice husk biomass with the natural mineral dolomite ($CaMg(CO_3)_2$) solution following pyrolysis step at 700 °C for 4 h at 8 °C $min^{-1}$. Pristine rice husk biochar (PRHB) was made by pyrolyzing rice husk for 4 h at 700 °C. The DRHB and PRHB were characterized via different techniques including, Fourier transform infrared spectroscopy (FTIR), thermogravimetric analysis (TGA) and Scanning electron microscopy (SEM). Afterwards, DRHB was used to get rid of the dyes in the wastewater solutions, and the effects of dose, pH, and contact duration were studied. Both RBB and RB-5 exhibited maximal adsorption capacities of 52.07 and 35.518 mg/g at 50 °C, respectively, and the findings matched well with the Langmuir model, demonstrating monolayer adsorption. For this system, the pseudo-second-order fit is optimal, pointing to chemisorption of both substances. The outcomes presented higher adsorption for RBB (95.63%) compared to RB-5 (85.20%) at 70 mg/L concentration, pH 6, 4 hr. contact time, and 0.3 mg of DRHB dosage. The primary mechanism to remove of both dyes was chemisorption via π-π bond and hydrogen bond. These findings provide insights to build an economical, and sustainable anionic dyes removal technique especially for the third world nations.


## 1. Introduction

William Henry Perkin originally revealed the dye in 1856, and since then, several variations on the original dye have been developed for application in different industries (Aracagök 2022). Dyes can be classified as either non-ionic (disperse), anionic (reactive, acidic, and direct), or cationic (basic) and most dyes are composed of aromatic structures (Hassan and Carr 2018, Al Kausor et al., 2022). The dyes gave our world a colorful appearance and were used mostly in the sectors of painting, textile manufacturing, tanning, dying, pharmaceutics, and paper and pulp production (Mittal 2021). Annually, the textile industry consumes 10,000 tons of dyes, generates 3,600 tons of wastes

* Corresponding author.
E-mail address: e.hassan@msstate.edu (E. Barbary Hassan).
Peer review under responsibility of King Saud University.

Production and hosting by Elsevier

https://doi.org/10.1016/j.arabjc.2023.105125
1878-5352 

containing dye, and discharges 5,000 tons of dye into wastewater effluents (Murugesan et al., 2021, Renita et al., 2021, Uddin et al., 2021). The dye use is surged in Asia, particularly in India and China. It is predicted that by the year 2030, 47% of the global population would have limited access to safe drinking water (Islam et al., 2021). Dye in water, even at concentrations as low as 1 mg/L, is incredibly unappealing (Ardila-Leal et al., 2021, Kapoor et al., 2022). Water transparency isn't the only thing the dyes interfere with; they also elevate turbidity, bacterial oxygen demand (BOD), chemical oxygen demand (COD), change the pH, and obstruct the light that would normally reach the water, which may reduce photosynthesis and hasten eutrophication (Hassan and Carr 2018, Wanyonyi and Mulaa 2020).

The usage of reactive dyes is exceptionally prevalent as they account for 45% of total dye use (Gokulan et al., 2019). The azo dyes are used widely (70% of the total dye's usage) due to their prominent characteristics such as high solubility, jet blackness and no dust formation (Feng et al., 2022). Reactive black 5 (RB-5) is an azo reactive dye with widespread use in the textile industry. Removal of RB-5 in the standard biological treatment stage is challenging since it is difficult to metabolize the dye and it cannot be digested in aerobic conditions (Salleh et al., 2011, Uddin et al., 2021). The presence of one or more diazinyl functional groups makes azo dyes highly resistant of photocatalysis and oxidizing agents (Ben Ayed et al., 2022). The azo bonds makes it carcinogenic and mutagenic to living organisms (Srivastava et al., 2022). The RB-5 was found to disrupt the zebrafish embryo (Namasivayam et al., 2018), the human neurological system, the digestive system, and induce skin allergy, confusion, headache, elevated blood pressure, and nausea, etc. (Munagapati et al., 2020, Kapoor et al., 2022). The dyes accumulate in aquatic creatures via the food chain, altering their metabolic rate and causing mortality in certain cases (Feng et al., 2022). Remazol brilliant blue (RBB), commonly known as Reactive blue-19, is a notable reactive dye that is a vinyl sulfone-based formazan dye (Arya et al., 2020). The textile sector is the principal consumer of RBB, which is utilized primarily as a starting material in the production of polymers (Raj et al., 2021). Like RB-5, RBB can cause cancer, alter genetic makeup, harm the eye, heart, kidney, lungs, liver and spleen, necrosis, jaundice, etc. (Aracagök 2022, Zhang et al., 2022).

The layered double hydroxides (Mittal 2021), metal–organic frameworks (Uddin et al., 2021), coagulation/flocculation (Sonal et al., 2018), clay minerals (Al Kausor et al., 2022) and ion exchange (Hassan and Carr 2018), electrochemical methods (Nidheesh et al., 2018), membrane technologies (Ahmed et al., 2021), bioremediation (Ihsanullah et al., 2020), ozonation (Elsayed et al., 2022) are energy demanding and costly techniques. Adsorption has emerged as a preferred method for treating wastewater due to its effectiveness, widespread acceptance, low cost, and minimal effect on the environment. The conversion of biomass into biochar is an inexpensive and sustainable technique due to the high accessibility of large number of feedstocks and non-toxicity (Madduri et al., 2020, Steigerwald and Ray 2021). Following this technique, the agricultural waste materials can be converted into biochar which is an efficient waste management technique and also contributes to climate change mitigation by carbon sequestration (Cheng et al., 2021, Kamali et al., 2021). Changing biochar's properties via modification may boost its adsorption capacity even further (Amen et al., 2020, Qiu et al., 2021). The modification can be a costly process, but the use of natural minerals for the modification is extremely simple and cost-effective technique which could assist in the large-scale application of biochar for the wastewater treatment (Li et al., 2019).

The biochar is usually considered as an anionic adsorbent due to abundance of humic and fulvic acids and presence of carboxylic and phenolic functional groups (Ren et al., 2015). This property makes biochar an unsuitable candidate for the absorbance of anionic pollutants. To solve this issue, several modifications have been done by different scientists. (Nguyen et al., 2021) used modified biochar with $CaCl_2$, $FeCl_3$ and $AlCl_3$ for the elimination of an anionic Congo red dye. (Zhang et al., 2014) used $MgCl_2$ and $Na(OH)_2$ for the wheat straw biochar modification for the adsorption of direct frozen yellow. In another study $MgCl_2$ was used to modify the biochar (Xu et al., 2018). However, the published studies on loading technique of Mg and Ca onto biochar is rather inconvenient and demands a substantial volume of reagent.

To ease the process, in this study, the pre-modification of rice husk has been done using a natural mineral "dolomite ($CaMg(CO_3)_2$" following the subsequent pyrolysis step (700 °C) for the biochar fabrication(DRHB). The DRHB was applied for the removal of RBB and RB-5 anionic dyes from the synthetic wastewater and examined the influence of dosage, pH, initial concentrations (adsorption isotherm) and contact time (kinetic study). Eventually, the adsorption mechanisms and regeneration potential of DRHB were investigated.

## 2. Materials and methods

### 2.1. Materials

Analytical-grade chemicals were employed in this investigation. Remazol Brilliant Blue ($C_{22}H_{16}N_2Na_2O_{11}S_3$, Sigma-Aldrich, CAS: 2580–78–1, MW: 626.54), Reactive Black 5 ($C_{26}H_{21}N_5Na_4O_{19}S_6$, Sigma-Aldrich, CAS: 17095–24-8, MW: 991.8), hydrochloric acid and sodium chloride were obtained from Sigma Aldrich. Both dyes' molecular structures are depicted in Fig. 1. The highly pure distilled water (DI) (17.8 megaohm) was used for all experiments. One gram of RB-5 and 1 g of RBB were each dissolved in one liter of DI to create a 1 g/L stock solution. The stock solutions were diluted to further use in the different parts of experiment. Solution pH was controlled using 0.1 M HCl and NaOH.

### 2.2. Biochar fabrication

The 15 g of rice husk biomass was placed in alumina crucible boat and pyrolyzed at 3 different temperatures 300, 500 and 700 °C in a furnace tube (OTF-1200X) for 4 h at heating rate of 8 ∘C $min^{-1}$ in presence of $N_2$ to obtain pristine rice husk biochar (PRHB). Based on high surface area, we choose to fabricate the DRHB at 700 °C using pre-modification technique. For pre-modification, 15 g of rice husk biomass was first immersed in the dolomite slurry (3 g Dolomite into 150 mL DI water) for 24 h following 1 h of sonication. The obtained biomass has been dried in an oven at 85 °C for 12 h. After that the biomass was placed in alumina crucible boat and pyrolyzed at 700 °C for 4 h at heating rate of 8 ∘C $min^{-1}$ in a furnace tube (OTF-1200X) under $N_2$.

### 2.3. Biochar characterization

The biochar was grinded to make homogenous powdered form. The FTIR spectrometer (Thermo Scientific Nicolet IS50) was used in the range of 400 to 4000 $cm^{-1}$ to examine functional groups of biochar. The carbon, nitrogen and hydrogen content of biochar was determined by using CE-440 Elemental Analyzer. The surface area and pore volume were examined using Quantachrome Autosorb iQ gar sorption analyzer (Quantachrome ASIC0500-5, USA). The DRHB structure was observed before and after the trial via FE-SEM (JEOL JSM-6500F Field Emission Scanning Electron Microscope).

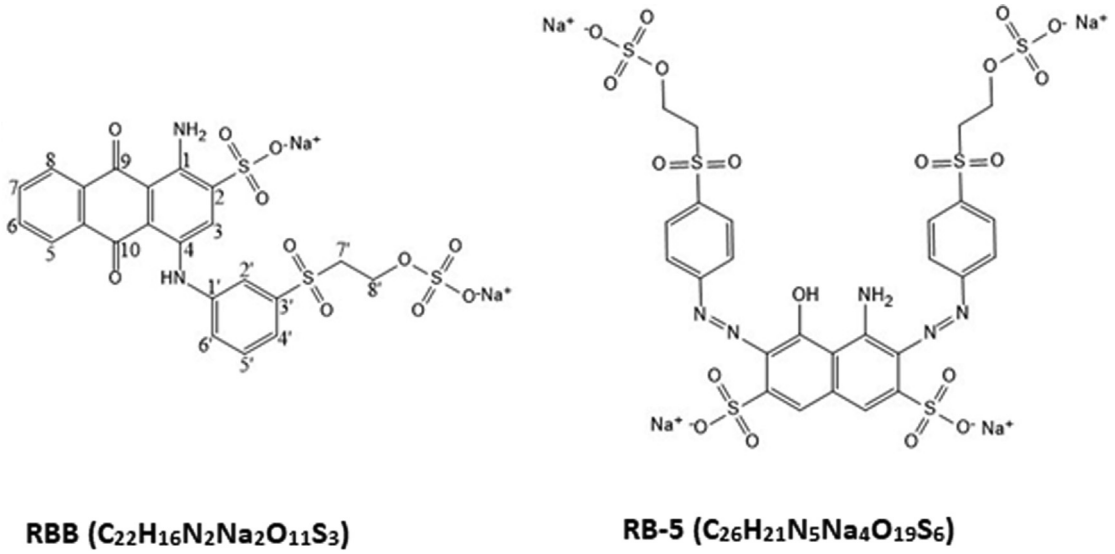


**Fig. 1** Chemical structures and empirical formulas of RBB and RB-5 dyes.

### 2.4. Point of zero charge (PZC)

To determine DRHB's PZC, 25 g of biochar was dissolved in 25 mL of 0.01 M NaCl solution. Using 0.1 M NaOH or HCl, the solution's pH was pre-set at 2, 4, 6, 8, 10, and 12. There was a 24-hour period of shaking the samples at 250 rpm. After then, the PZC was calculated based on the final pH plot.

### 2.5. Adsorption experiments

#### 2.5.1. Influence of pH

The pH effects on adsorbate adsorption potential were studied by varying the pH from 2 to 12 at 2-point intervals. The 20 mg of adsorbent was added into 20 mL of 70 mg/L RB-5 and RBB solution and agitated at 250 rpm for 4 h. Initially, dissolved $CO_2$ was removed from the NaCl solution by purging the system with $N_2$ gas. The 0.22 m syringe filters were used to filter the final product and placed in the vials for further concentration analysis.

#### 2.5.2. Adsorption kinetics

The adsorption kinetics for RB-5 and RBB removal using DRHB was determined. The 30 mg of biochar was added in 10 mL solution of 30, 50 and 70 mg/L of RB-5 and RBB solution having pH 6 and agitated in mechanical shaker at 250 rpm speed for time ranging from 10 min to 360 min. A syringe filter with a pore size of 0.22 μm was used to filter the solution before continuing the study. Adsorption kinetics for RB-5 and RBB on DRHB were studied using linear and non-linear pseudo-first order and pseudo-second order models.

The following equation was used to determine the removal efficiency:

$$\%removal = \left(\frac{C_0 - C_e}{C_0}\right) * 100 \quad (1)$$

The following equation was used to determine the sorption capacity:

$$qt = \frac{(C_0 - C_t)V}{m} \quad (2)$$

$C_0$ is the initial concentration (mg/L) of dyes, $C_t$ is the dyes concentration at time t (mg/L), V is solution volume (L), m is adsorbent mass (g).

Thermodynamics study has been done at 25, 35 and 50 °C using 0.3 g biochar, 70 mg/L of RB-5 and RBB solutions (10 mL) to examine the temperature influence and energy changes during the adsorption using Van't Hoff equation:

$$\Delta G = -RTlnK_d \quad (3)$$

$$lnK_d = \frac{-\Delta H}{RT} + \frac{\Delta S}{R} \quad (4)$$

$$K_d = \frac{q_e}{C_e} \quad (5)$$

The T is the absolute temperature in Kelvin, R is equal to 8.314 J $K^{-1}$ (Gas constant), $K_d$ is distribution coefficient, $\Delta G$ is heat capacity in kJ.$mol^{-1}$, $\Delta S$ is entropy in J.$mol^{-1}K^{-1}$, $\Delta H$ is enthalpy in KJ.$mol^{-1}$.

#### 2.5.3. Adsorption isotherms

The isothermal study of both dyes, RB-5 and RBB was conducted using the dye concentration ranging from 20 to 140 mg/L in 10 mL solution, 30 mg of DRHB dosage, 3 different temperatures (25, 35 and 50 °C) and the shaking speed was 250 rpm was used. The linear and non-linear Langmuir and Freundlich isotherm models were used to fit the adsorption data of RB-5 and RBB adsorption on DRHB. The equations for both pseudo kinetic orders and isotherm models are presented in Table 1.

The blank without any dye was run before making the standard calibration curve for each dye on UV–Vis Spectrophotometer (Azzota SM-1800). The instrument was set to measure the light at a wavelength of 593 nm for RBB and 597 nm for RB-5. After making standard curve in range of 5 to 50 mg/L, the dye concentration was evaluated after each adsorption trial.

**Table 1** List of adsorption isotherms and kinetic models.

| Model | Equation |
|---|---|
| Langmuir linear | $\frac{Ce}{qe} = \frac{1}{Klqmax} + \frac{Ce}{qmax}$ |
| Langmuir non-linear | $Qe = \frac{QmKlCe}{1+KlCe}$ |
| Freundlich linear | $\ln(qe) = [\ln(Kf) + (\frac{1}{n})\ln(Ce)]$ |
| Freundlich non-linear | $Qe = KfCe^{1/n}$ |
| Pseudo first order non-linear | $Qt = Qe(1 - e^{-k1t})$ |
| Pseudo first order linear | $\log(qe - qt) = [\log(qe) - (\frac{k1}{2.303}) \times t]$ |
| Pseudo second order non-linear | $Qt = \frac{k2tQe^2}{1+k2tQe}$ |
| Pseudo second order linear | $\frac{t}{qt} = \frac{1}{k2(qe)^2} + \frac{t}{qe}$ |

### 2.6. Regeneration experiment

Biochar was tested for its reusability by performing sorption/desorption studies. Initially, the desorption capability was investigated using HCl of 0.1 M and NaOH 0.1 M. The NaOH exhibited more efficacy in regeneration of both dyes RB-5 and RBB compared to HCl due to same anionic charge. The regeneration experiment was performed using 0.3 g biochar, 70 mg/L of RB-5 and RBB solutions, following by washing using10 mL of 0.1 M NaOH for 60 min for three cycles. The desorption % of DRHB for both dyes was determined using following equation:

$$\%Desorption = \left(\frac{C_0 des}{C_{sorb}}\right) * 100 \quad (6)$$

$C_0$ represents the initial dye concentration in mg/L, and $C_{sorb}$ represents the final dye concentration after sorption.

## 3. Results and discussions

### 3.1. Evaluation of pH effect and point of zero charge (PZC)

The pH of solution and the adsorbent type both are significant parameters influencing sorption of contaminants. The DRHB showed higher removal efficiency for both dyes (RBB and RB-5) at acidic pH compared to the alkaline (Fig. 2). At pH 2, the removal percentage for RBB and RB-5 was 99.39% and 96.922%, respectively. Till pH 6 the removal percentage was high for both dyes after which a clear decline in the adsorption potential was detected with lowest removal percentage for both dyes RBB and RB-5 (64.25% and 49.43%) at pH 10 (Fig. 2). Dye adsorption is influenced by dye ionic form and charge on the DRHB surface at different pH levels. Both dyes are anionic in nature and exhibited higher adsorption potential in acidic pH because of the electrostatic attraction after the protonation of surface functional groups of DRHB. The negatively charged functional groups on the DRHB surface, as well as an abundance of OH– groups, prevent the sorption of alkaline dyes in an alkaline environment owing to electrostatic repulsion. In case of RBB, the $H^+$ interacts with the $NH_2$ group on carbon 1 of the third ring of dye and transforming it into protonated $NH_3$ in acidic conditions (Mahmoud et al., 2007). The overall mechanism is explained in below equations (7) and (8):

$$C_{22}H_{16}N_2Na_2O_{11}S_3 + H^+ \rightarrow [C_{22}H_{17}N_2Na_2O_{11}S_3]^+ \quad (7)$$

$$[C_{22}H_{17}N_2Na_2O_{11}S_3]^+ \rightarrow [C_{22}H_{15}N_2Na_2O_{11}S_3]^+ + H_2 \quad (8)$$

This results in increase in the adsorption at cation exchange sites causing high removal in acidic pH and the adsorption drops dramatically when the pH rises over 7. Both dyes possess $SO_3^-$ groups which facilitates the electrostatic interaction in the acidic environment. (Arya et al., 2020) and (Nandanwar et al., 2022) observed similar outcomes of pH influence on RBB adsorption on carbon-based adsorbents. In alkaline condition the, the dye loses one $H^+$ which reacts with $OH^-$group in the alkaline solution to form water. The outcome of losing $H^+$ is the development of negative charge on the carbon # 7 of the dye solution resulting in $[C_{22}H_{15}N_2Na_2O_{11}S_3]^-$, as shown in equation (9). When electrons are transferred from the adjacent sulfonyl group to carbon # 7′, a sulfur carbon double bond (S = C) develops, and the oxygen atom of the sulfonyl group acquires a negative charge (Nagendrappa 2004, Mahmoud et al., 2007).

$$C_{22}H_{16}N_2Na_2O_{11}S_3 + OH^- \rightarrow [C_{22}H_{15}N_2Na_2O_{11}S_3]^- + H_2O \quad (9)$$

The high removal of RB-5 and RBB in acidic environment might be due to the electrostatic attraction due to the opposite charges. The removal of anionic dyes at alkaline pH might be

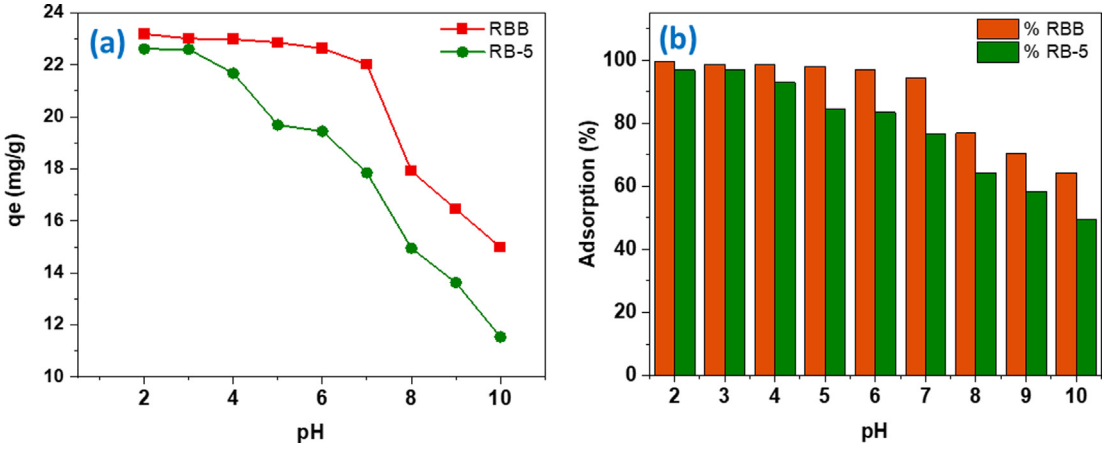


**Fig. 2** Influence of pH on the removal performance of DRHB for RBB and RB-5 dyes (a) Adsorption capacity (mg/g) and (b) Adsorption (%).

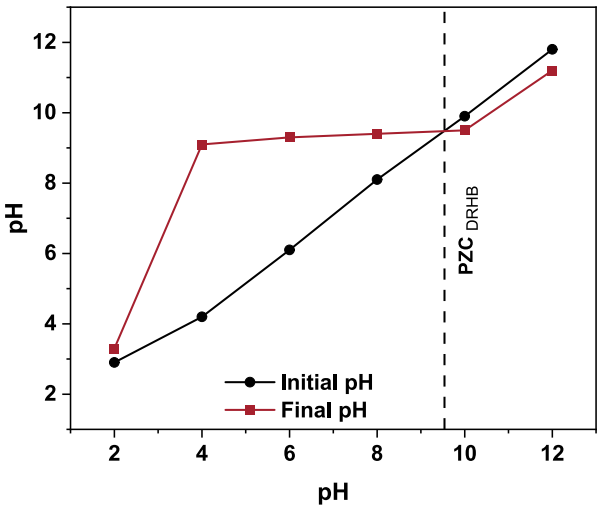


**Fig. 3** Point of zero charge (PZC) of DRHB.

due to the chemisorption and pore diffusion mechanism. The point of zero charge (PZC) of adsorbent surface also plays crucial role in adsorption mechanism of dyes. The experiment outcomes depicted the pzc of DRHB is 9.5 (Fig. 3). At this value, the net surface charge of biochar is zero. Furthermore, pyrolysis temperature has an important role in determining pzc value. Biochar fabricated at high temperature (700 °C) has high pzc values due to the formation of inorganic carbonates $Mg^{2+}$ and $Ca^{2+}$ (Yuan et al., 2011, Bombuwala Dewage et al., 2019). An abrupt increase in the pH of final solution from 2 to 4 has been observed which could be attributed to dissolution of dolomite at acidic pH results in the release of carbonates ions which increase pH. Dolomite also possesses $Ca^{2+}$ and $Mg^{2+}$ ions which is also the reason for the high pzc of DRHB.

### *3.2. Characterization of PRHB biochar and DRHB*

SEM micrographs display the morphology and structure of the fabricated PRHB, DRHB and DRHB after adsorption (Fig. 4). The surface of PRHB looked smooth and more porous with some impurity particles. However, the structural changes in the DRHB have been clearly noticeable due to the modification. The DRHB surface appeared rough and pores appeared to be filled due to the even distribution of dolomite over its surface. The outcomes of BET analysis support it as the surface area of PRHB is higher (238.54 $m^2/g$ compared to the DRHB (214.24 $m^2/g$) (Table 2) (Li et al., 2019). The DRHB surface after adsorption seemed to be loaded with dyes

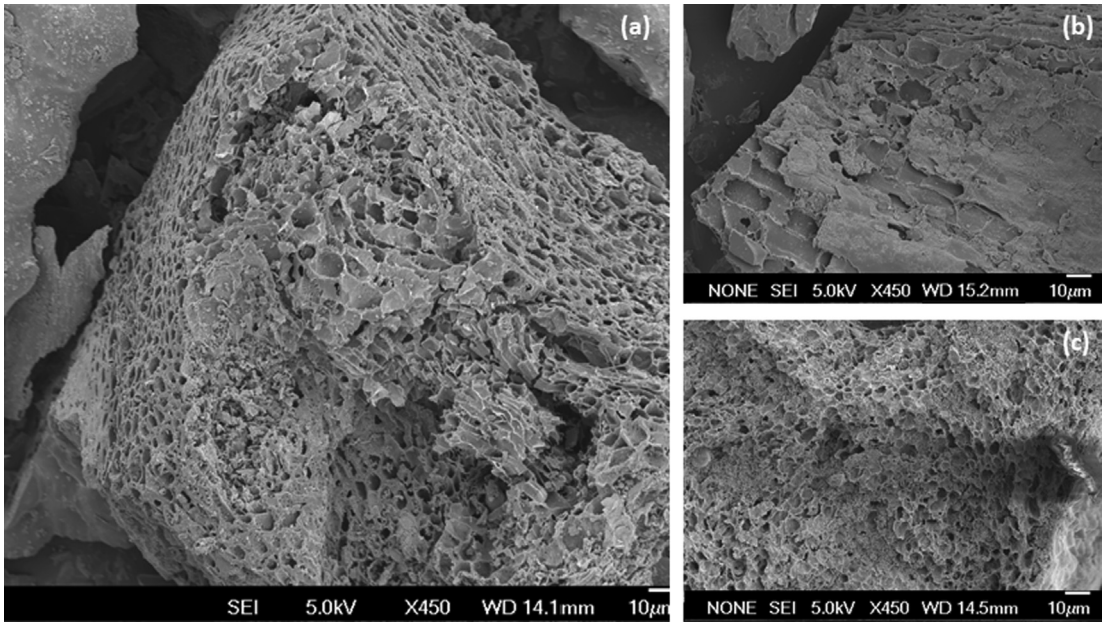


**Fig. 4** Fe-SEM micrograph of (a) PRHB, (b) DRHB and (c) DRHB after adsorption.

**Table 2** Elemental analyses and surface area of PRHB and DRHB.

| Sample | Pyrolysis temperature (°C) | Elemental analysis | | | | Surface area |
|---|---|---|---|---|---|---|
| | | C% | H% | N% | R% | $m^2/g$ |
| PRHB | 300 °C | 44.09 | 4.17 | 0.76 | 50.98 | 73.70 |
| PRHB | 500 °C | 46.28 | 2.11 | 1.08 | 50.53 | 113.48 |
| PRHB | 700 °C | 47.64 | 1.46 | 1.83 | 49.07 | 238.54 |
| DRHB | 700 °C | 41.63 | 1.26 | 1.03 | 56.09 | 214.24 |

and crushed due to vigorous stirring during the experimentation.

EDX spectral examination of the adsorbent surface indicated several elements including C, O, Ca, Mg, N and Cl, etc. The detection of magnesium and calcium in EDX spectra validates the successful modification of biochar (Fig. 5a, b). According to the $N_2$ adsorption–desorption isotherm, biochar has a curve that is characteristic of Type IV isotherms and hysteresis H3. Capillary condensation in mesoporous materials causes this hysteresis. The Type IV isotherm may be divided into two branches, the first of which corresponds to monolayer $N_2$ adsorption and the second of which is linked to the formation of multilayers (Fig. 5c) (Silva et al., 2016).

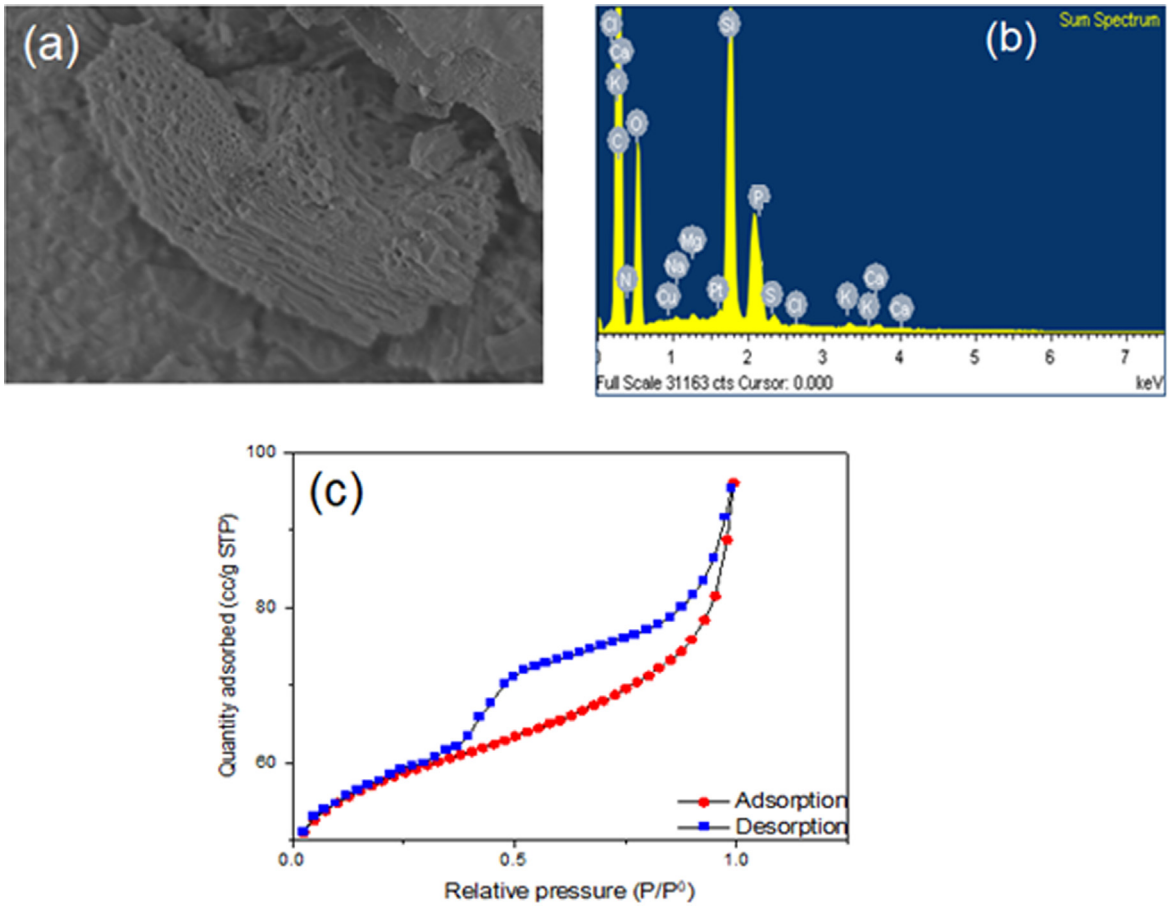


**Fig. 5** Electron Image and EDS spectra of DRHB (a, b) and nitrogen adsorption–desorption analysis of DRHB (c).

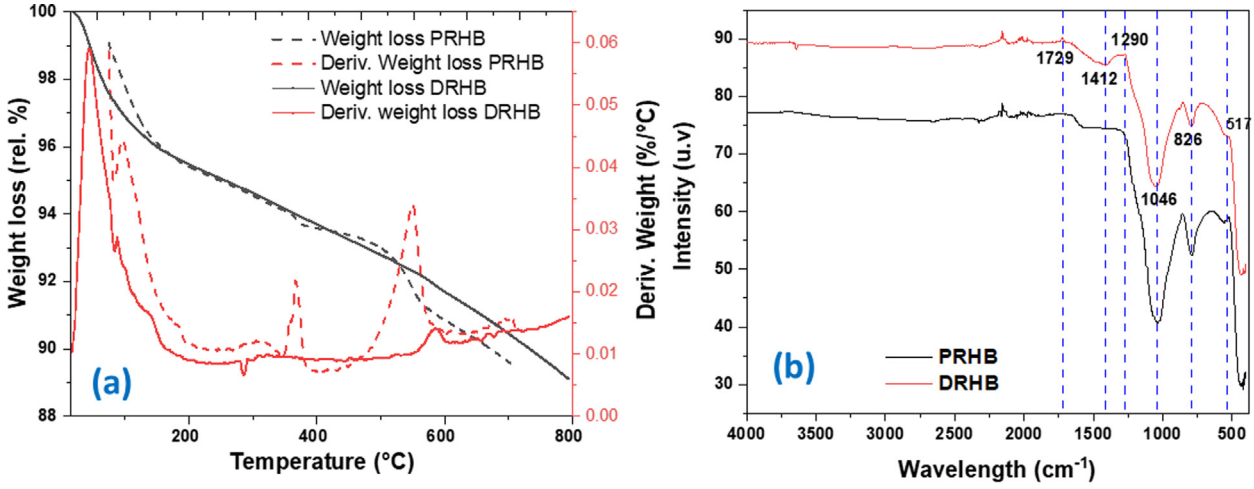


**Fig. 6** (a) TGA-DTG thermograph of PRHB and DRHB (b) FTIR spectra of PRHB and DRHB.

**Table 3** Adsorption Kinetic parameters for RBB and RB-5 at initial concentration of 30, 50 and 70 (mg/L), 0.03 (g/L) DRHB dosage and temperature 25 °C.

| Models | $C_o$ (mg/L) | RBB | | | RB-5 | | |
|---|---|---|---|---|---|---|---|
| | | 30 | 50 | 70 | 30 | 50 | 70 |
| Pseudo-first order | $K_1$ (1/min) | 0.053 | 0.041 | 0.062 | 0.044 | 0.034 | 0.016 |
| | $q_e$ (mg/g) | 9.60 | 15.017 | 20.923 | 9.761 | 13.89 | 19.163 |
| | $R^2$ | 0.95 | 0.911 | 0.922 | 0.949 | 0.947 | 0.958 |
| Pseudo-second order | $K_2$ (g/mg/min) | 0.008 | 0.005 | 0.004 | 0.007 | 0.004 | 0.005 |
| | $q_e$ (mg/g) | 10.34 | 16.12 | 22.47 | 10.49 | 14.99 | 20.48 |
| | $R^2$ | 0.996 | 0.987 | 0.993 | 0.986 | 0.992 | 0.998 |

The thermogravimetric analysis (TGA) of PRHB and DRHB is displayed in Fig. 6a. Different endothermic weight losses are observed at different temperatures for both biochars. The sharp 5% weight loss is observed till 150 °C for PRHB and 3% observed at temperature of 100 °C which is attributed to the moisture loss (Eltaweil et al., 2020). Sharp decrease in weight loss is observed from 150 to 800 °C for PRHB which might be due to the decomposition of organic compounds, including lignin and cellulosic compounds (Eltaweil et al., 2022). From 100 to 560 °C the weight loss trend was stable and after that a rapid loss in weight was observed which can be due to the decomposition of $H_2$, carbonates and organic compounds. The peak at 800 °C might be ascribed to structural carbon breakage (do Nascimento et al., 2021). The weight loss of DRHB is less as compared to PRHB specifically from 350 to 620 °C which can be due to presence of magnesium and calcium, both have high melting points.

The FTIR spectra provides insight into the available functional groups in adsorbent to understand the adsorption mechanism (Fig. 6b). The peaks shoulder like peaks from 427 to 827 $cm^{-1}$ represents $–OCH_3$ aromatic band. The bending peak at 1046 $cm^{-1}$ confirms the presence of Si-O-Si and C-O-C functional groups (Singh et al., 2022). The bending at 1290 $cm^{-1}$ represents the C-N amide III. The peak at 1412 $cm^{-1}$ in DRHB is due to the stretching of -C = O group representing the inorganic carbonates which is a proof of successful modification with dolomite (Mecozzi et al., 2012). Functional groups like aromatic C = C stretching vibrations may be identified in the FTIR spectrum at about 1600 $cm^{-1}$. The concentration of this band in the PHRB was slightly higher than that in the DHRB. The stretching of C = O in aromatic groups represented small bend at 1729 $cm^{-1}$ in both biochars (Fig. 5b). The vibration bands between 400 and 800 $cm^{-1}$ identifies the Mg-O and O-Mg-O groups (Fang et al., 2015, Li et al., 2019). The slight peaks from 1500 to 2300 $cm^{-1}$ represent the C–H vibrations of aliphatic groups. The results obtained from FTIR analysis indicate that the surface of biochar contains various functional groups such as carbonyl, aromatic, aliphatic, carboxyl, hydroxyl, and amide functional groups.

### 3.3. Adsorption study

#### 3.3.1. Adsorption kinetic

For process optimization and scaling up investigations, kinetic models are helpful because they can depict the operation of the batch sorption system under different experimental settings. In this investigation, the sorption rates of RBB and RB-5 were assessed using the pseudo-first order and pseudo-second order kinetic models. The pseudo-second order $R^2$ value for both RBB and RB-5 spanned from 0.98 to 0.99. The $R^2$ value of pseudo-first order for RBB ranges from 0.91 to 0.95 and 0.94 to 0.95 for RB-5. The $q_e$ of DRHB for RB-5 spanned from 10.49 to 20.48 mg/g and 10.34 to 22.47 mg/g for RBB (Table 3, Fig. 7). Pseudo-second order model was found to be the best match for the data, and this model indicates that adsorption rate is independent of adsorbate concentration and instead is proportional to adsorbent capacity. Moreover, this demonstrates that chemisorption is the rate-limiting phase in this experiment (Sahoo and Prelot 2020, Xu et al., 2021). In chemisorption, the adsorbate reacts with adsorbent through chemical bond. The precipitation or bonding of both dyes with MgO and CaO plays key role in regulating the adsorption process and the molecules of both dyes could be adsorbed via intermolecular forces on the exterior surface of DRHB as shown in the removal mechanism Fig. 11.

After 180 min, the adsorption equilibrium was attained for all three concentrations at 30, 50 and 70 (mg/L) yielding highest removal from 95.63 to 100% for RBB and 85.20 to 100% for RB-5. The association between the adsorption of dyes (RBB and RB-5) and contact time is exhibited in Fig. 8. The DRHB removed 100% of RBB and RB-5 at 30 mg/L after 240 min. After 4 h the further contact time was showing negligible efficiency in removing both dyes RBB and RB-5. The kinetic results suggested that the removal efficiency seemed to be increased with the contact time, but desorption began after the 6-hour contact period, which may have been caused by the biosorbents maximal affinity and the achievement of equilibrium. The initial fast adsorption is ascribed to the high availability of active sites (Huang et al., 2018). At beginning the dye molecules attached to the DRHB surface via electrostatic attraction, van der waals forces, hydrogen bonding and surface complexation, following the diffusion (surface and intra-particle diffusion). The prolonged contact time could increase the likelihood of desorption as the system will have more time to reach equilibrium. The denseness of dyes molecules in biochar elevates diffusion resistance which could cause desorption (He et al., 2019).

#### 3.3.2. Adsorption isotherms

The correlation between equilibrium adsorption capacity and initial concentration can be comprehended with the help of adsorption isotherms. Equilibrium adsorption is a crucial metric for providing an overview of the relationship between adsorbent and adsorbate (Reghioua et al., 2021). To determine the optimal adsorption equilibrium isotherm for dye removal

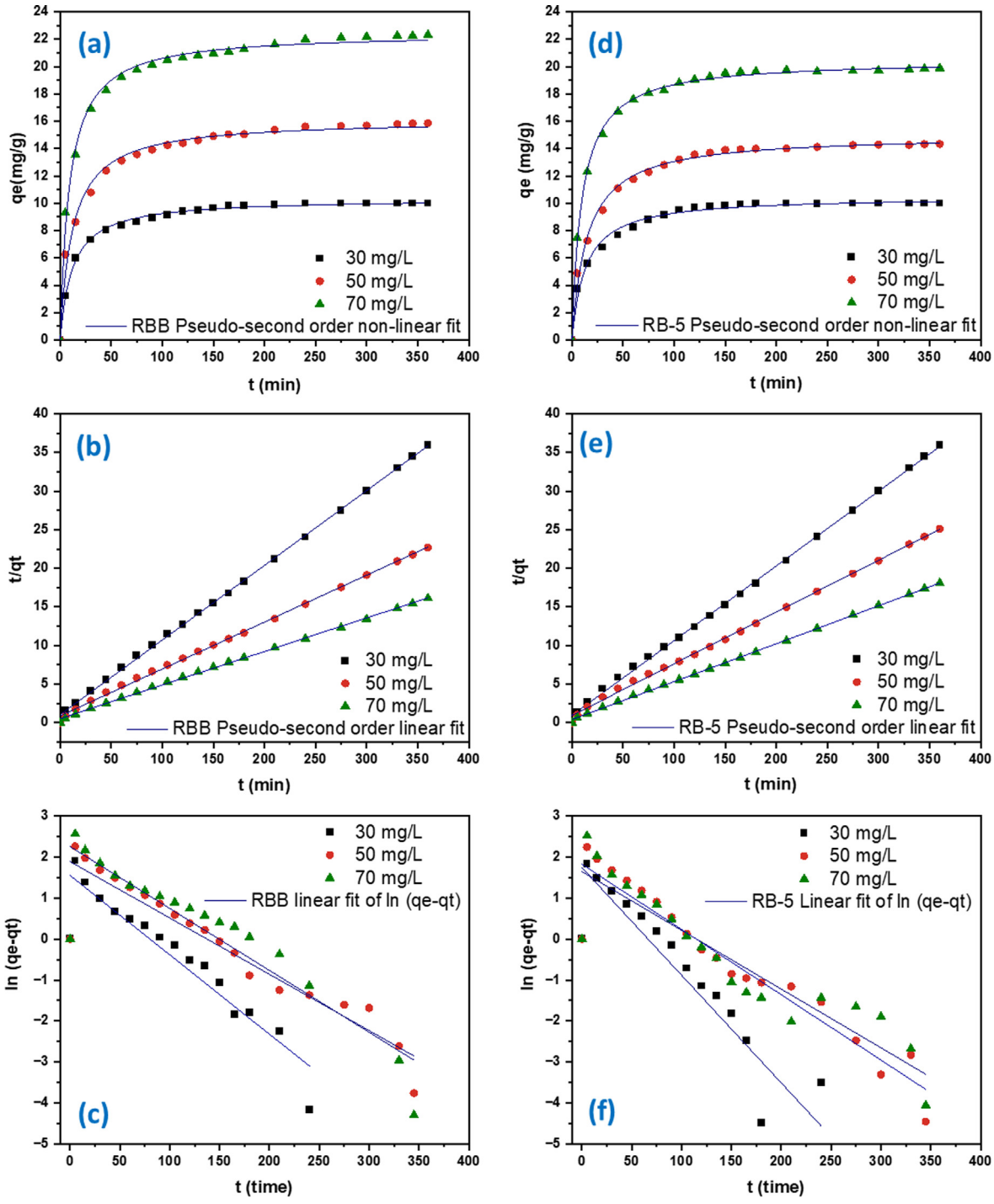


**Fig. 7** The adsorption kinetics of RBB using DRHB at 25 °C (a) RBB Pseudo-second order non-linear fit (b) RBB Pseudo-second order linear fit and (c) RBB Pseudo-first order linear fit (d) RB-5 Pseudo-second order non-linear fit (e) RB-5 Pseudo-second order fit and (f) RB-5 Pseudo-first order linear fit.

by DRHB and thus maximize the adsorption mechanism routes involved, it is essential to investigate several adsorption equilibrium isotherms. Langmuir and Freundlich are the most prevalent models for sorption experiments (Langmuir 1918).

The RBB and RB-5 were taken in different concentration ranges from 20 to 140 mg/L at three different temperatures 25, 35 and 50 °C. The $R^2$ value of Non-linear Langmuir isotherm of RB-5 spanned from 0.97 to 0.99 while for RBB all $R^2$ values were higher than 0.99. The overall highest $q_{max}$ values at three temperatures for RBB and RB-5 spanned from 32.77 to 52.07 mg/g and 22.84 to 35.518 mg/g, respectively (Table 4). Both RBB and RB-5 reached their maximal adsorp-

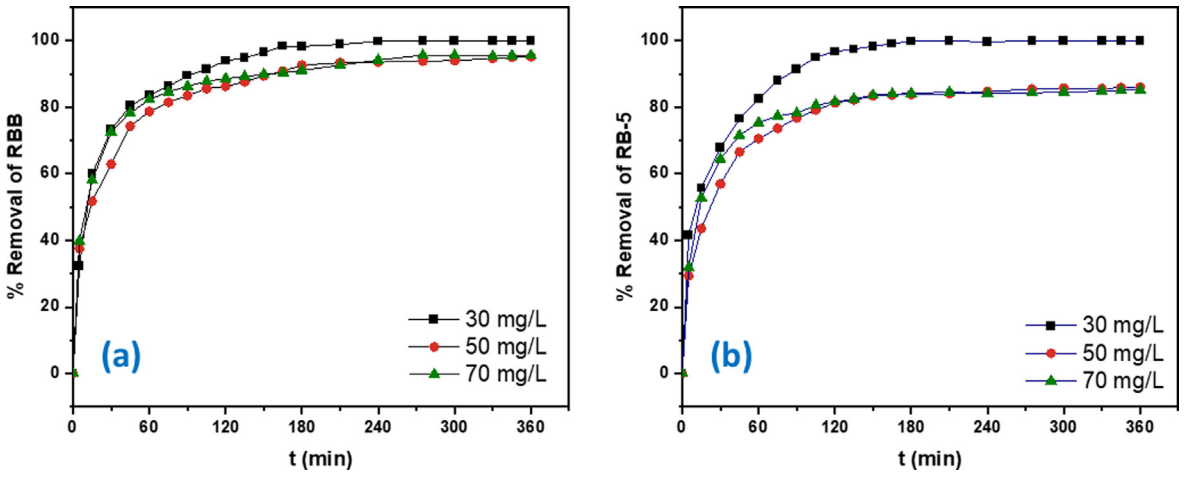


**Fig. 8** The removal % of (a) RBB and (b) RB-5 at different concentrations.

**Table 4** Langmuir and Freundlich isotherm model values for RBB and RB-5 at initial concentration from 20 to 140 (mg/L) and three different temperatures (25, 35 and 50 °C).

| Models | | RBB | | | RB-5 | | |
|---|---|---|---|---|---|---|---|
| | Temp (°C) | 25 | 35 | 50 | 25 | 35 | 50 |
| Langmuir | $K_1$ (L/mg) | 0.0417 | 0.127 | 0.208 | 0.1079 | 0.0777 | 0.1267 |
| | $q_{max}$ (mg/g) | 32.77 | 36.76 | 52.07 | 22.84 | 28.93 | 35.52 |
| | $R^2$ | 0.997 | 0.997 | 0.996 | 0.992 | 0.985 | 0.973 |
| Freundlich | $K_F$ ([mg/g(Lmg$^{-1}$)$^{1/n}$]) | 4.146 | 7.225 | 10.247 | 5.013 | 5.440 | 7.860 |
| | N | 2.065 | 2.59 | 2.93 | 3.08 | 2.63 | 2.72 |
| | $R^2$ | 0.951 | 0.950 | 0.979 | 0.936 | 0.922 | 0.913 |

tion potential of 52.07 and 35.518 mg/g at 50 °C, respectively (Fig. 9). The $R^2$ value of Freundlich isotherm spanned from 0.95 to 0.97 for RBB and 0.91 to 0.93 for RB-5. The $R^2$ value clearly shows that our experimental data follows Langmuir isotherm. Similar results are exhibited by different research studies for both dyes in which the data is well fitted to Langmuir isotherm (do Nascimento et al., 2021, Hii 2021, Nguyen et al., 2021, Parimelazhagan et al., 2022). The 50 °C proves to be the most favorable temperature for sorption of both dyes in this study. This finding confirms that DRHB's principal mechanism of dyes elimination is monolayer sorption.

The adsorption potential of different sorbents for RBB and RB-5 removal is presented in Table 5. Overall, the DRHB exhibited highest removal capacity for RBB (52.07 mg/g) as compared to the other cited literatures in Table 5 at pH 6. The Banana peel powder exhibited higher sorption value (49.2 mg/L) for RB-5 than DRHB (35.518 mg/L) that might be due to the highly acidic environment (Table 5) that limits there field applicability because the pH of textile water is mostly alkaline (Srivastava et al., 2022, Srivastava et al., 2022). The pH of working solution in our study is near to neutral, similar the real dye contaminated wastewater. The fabrication of biochar using agricultural waste and modification using natural mineral dolomite is a cheaper alternative to other sorbents. More research is needed to determine the monetary worth of dolomite-modified biochar for the treatment of different contaminants. The influence of different modification techniques e.g., post modification, can be done to evaluate the efficiency of dolomite modified biochar on anionic pollutants removal.

### 3.3.3. *Adsorption thermodynamics*

Adsorption thermodynamics is a subfield of thermodynamics that focuses on examining the state of equilibrium conditions and energy shifts linked to the adsorption process. This observation offers valuable insights into the interplay among adsorbent and adsorbate molecules, as well as the variables that impact the adsorption process. The ΔH° and ΔS○ was determined by using the slope and intercept after plotting graph between ln$K_d$ and 1/T Fig. 10. Table 6 showed the ΔH° values of both dyes (RBB and RB-5) are > 1 which indicates the adsorption process was endothermic, which is consistent with the increase in adsorption with temperature (Li et al., 2021). As RBB and RB-5 dyes had negative $G_o$ values (−0.46764, −1.89913 and −3.47033 KJ.mol$^{-1}$) and (−0.21402, −0.72404 and −2.12273 KJ.mol$^{-1}$) it was determined that biochar was successful in removing them spontaneously. The $G_o$ getting more negative with the increase in temperature indicates that higher temperature is more favorable for removing both dyes. The RBB and RB-5 both exhibited positive ΔS○ (119.366 and 77.16416 J.mol$^{-1}$.K$^{-1}$) values, indicating strong attraction between both dyes and DRHB.

### 3.3.4. *Adsorption mechanism*

Dye adsorption onto biochar is influenced by several variables, such as the surface's functional groups, porosity, adsorbate

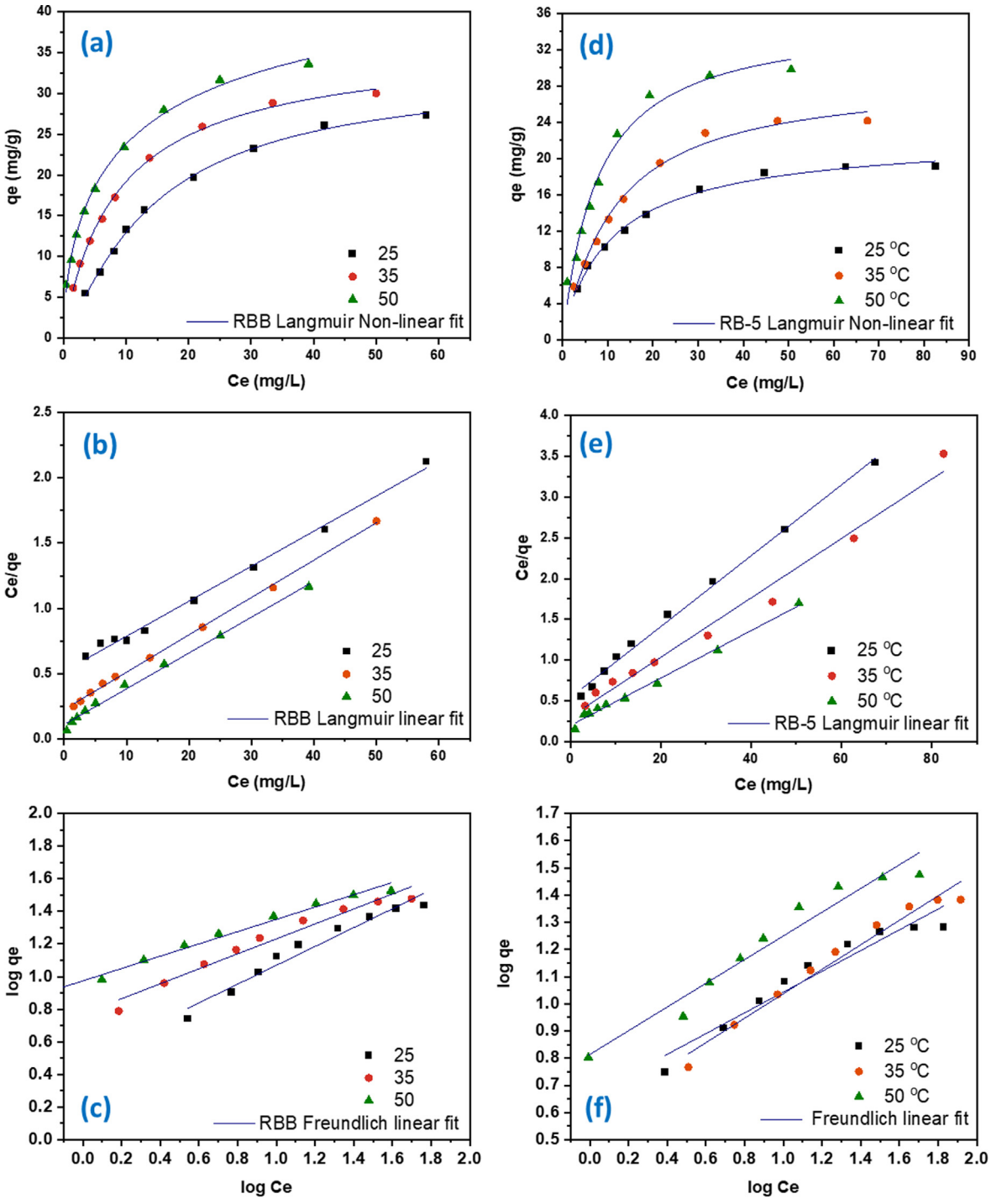


**Fig. 9** The Langmuir and Freundlich adsorption isotherm of RBB using DRHB (a) RBB Langmuir Non-linear fit (b) RBB Langmuir Linear fit (c) RBB Freundlich linear fit (d) RB-5Langmuir Non-linear fit (e) RB-5 Langmuir Linear fit (f) RB-5 Freundlich linear fit.

structure, concentration, solution pH and diffusion behavior. Knowing the adsorption mechanism is crucial for comprehending the RBB and RB-5 absorption onto the DRHB surface. The results from the characterization and sorption studies provides useful information regarding the adsorption mechanism (Fig. 11). The sorption study outcomes reveal that the adsorption is monolayer and mostly dependent on the chemical interactions. RBB and RB-5 contains sulfonic group which ionize in the form of colored anions after contact with water. Adsorption of both dyes is greatly influenced by the abundance of anions ($-SO_3^-$). The removal of both dyes is thus indicated to be mainly achieved by electrostatic attraction, π-π, and hydrogen bonding, especially at acidic pH levels in the presence of protonated surface functional groups on biochar (Dutta et al., 2021). The adsorption continues in the basic environment specifically due to the pore filling and diffusion mech-

**Table 5** Difference in adsorption capacity of various adsorbents for RBB and RB-5.

| Adsorbent | | pH | Qmax (mg/g) | Reference |
|---|---|---|---|---|
| Dolomite modified biochar | RBB | 6 | 52.07 | This study |
| Mesoporous activated carbon | | 2 | 33.47 | (Silva et al., 2016) |
| Activated charcoal | | 6 | 3.82 | (Arya et al., 2020) |
| Bone char | | 6.54 | 20.66 | (Bedin et al., 2017) |
| Pineapple leaf powder | | – | 9.6 | (Rahmat et al., 2016) |
| Hydrogel | | 6 | 9.88 | (Mate and Mishra, 2020) |
| Coconut shell activated carbon | | 6.5 | 35.08 | (Hii, 2021) |
| Coconut shells | | – | 8.01 | (Lai, 2021) |
| Dolomite modified biochar | RB-5 | 6 | 35.518 | This study |
| High lime fly ash | | 5.64 | 7.18 | (Eren and Acar, 2007) |
| Chitosan modified chloride moieties | | 3 | 7.956 | (Elwakeel, 2009) |
| Capuassu shell | | 2 | 22.9 | (Cardoso et al., 2011) |
| Magnetic iron oxide nano-particles | | 4 | 18 | (Chang and Shih, 2018) |
| Banana peel powder | | 3 | 49.2 | (Munagapati et al., 2018) |

**Table 6** The distribution and thermodynamic parameters calculated for the adsorption of RBB and RB-5 at different temperatures.

| Adsorbent | T (°C) | qe (mg/g) | $K_d = \frac{q_e}{C_e}$ | $lnK_d$ | ΔG° (KJ.mol$^{-1}$) | ΔH° (KJ.mol$^{-1}$) | ΔS° (J.mol$^{-1}$.K$^{-1}$) |
|---|---|---|---|---|---|---|---|
| RBB | 25 | 15.674 | 1.20773 | 0.1887476 | −0.46764 | 35.0179 | 119.366 |
| | 35 | 17.259 | 2.09938 | 0.7416418 | −1.89913 | | |
| | 50 | 18.322 | 3.64109 | 1.2922850 | −3.47033 | | |
| RB-5 | 25 | 14.806 | 1.09022 | 0.0863830 | −0.21402 | 22.87499 | 77.16415 |
| | 35 | 16.517 | 1.32677 | 0.2827498 | −0.72404 | | |
| | 50 | 17.373 | 2.20441 | 0.7904624 | −2.12273 | | |

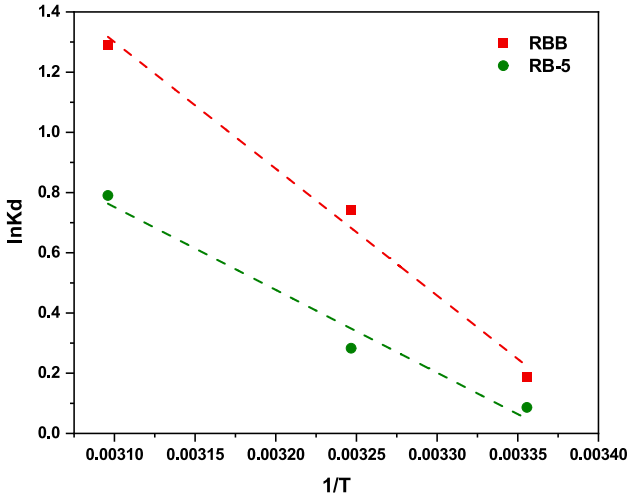


**Fig. 10** The linear diagram of Van't Hoff equation to calculate the thermodynamics parameters.

anism. Dye-biochar interactions include ligand exchange at the inner sphere and metal ion complexes at the outer sphere (Li et al., 2019).

Both dyes possess different functional groups including NH, C = O, S = O and $NH_2$ which are accessible for making bonds with –CH, –OH, and –CO groups on DRHB surface via hydrogen bonding, π-π, ion-exchange and electrostatic attraction. Dye sorption on the DRHB surface is facilitated in the presence of $Ca^{2+}$ due to the development of ternary complexes through metal-bridging. It has been observed that mineral ions ($Mg^{2+}$ and $Ca^{2+}$) in biochar are displaced during the elimination of both dyes due to the exposure of biochar surface to the aqueous solution. The anion exchange process contributes in the removal of both dyes as a result of the discharge of cations (such as calcium and magnesium) and anions (such as $SO_4^{2-}$, $NO_3^-$, etc.) from biochar surface which make it quicker for dyes containing sulfonic groups to interact with cations on the surface of the biochar (Singh et al., 2022).

### 3.4. Recyclability

Biochar-based materials can be used practically and economically after undergoing a particular amount of sorption/desorption cycles. To assess the regenerative potential of DRHB, the experiment was performed using DRHB by adsorbing and desorbing RBB and RB-5 in 3 regeneration cycles using 0.1 M NaOH. The adsorption % of DRHB for RBB in three cycles was from 65.31% to 94.28%. The adsorption % of RB-5 by DRHB was less compared to RBB. After the first cycle, the RB-5 adsorption % reduced to 74.36% and 58.39% after the third cycle. The removal % of RBB and RB-5 from DRHB in the first cycle was 86.16 and 85.34% for RBB and RB-5, respectively. Even after the third cycle the 62.422 and 43.714% of RBB and RB-5 was removed from DRHB (Fig. 12). The decrease in the adsorption rate after each cycle might be attributed to the structural and chemical changes (changes in functional groups) in the biochar due to treatment with NaOH. Also, after each cycle some dyes molecules remain

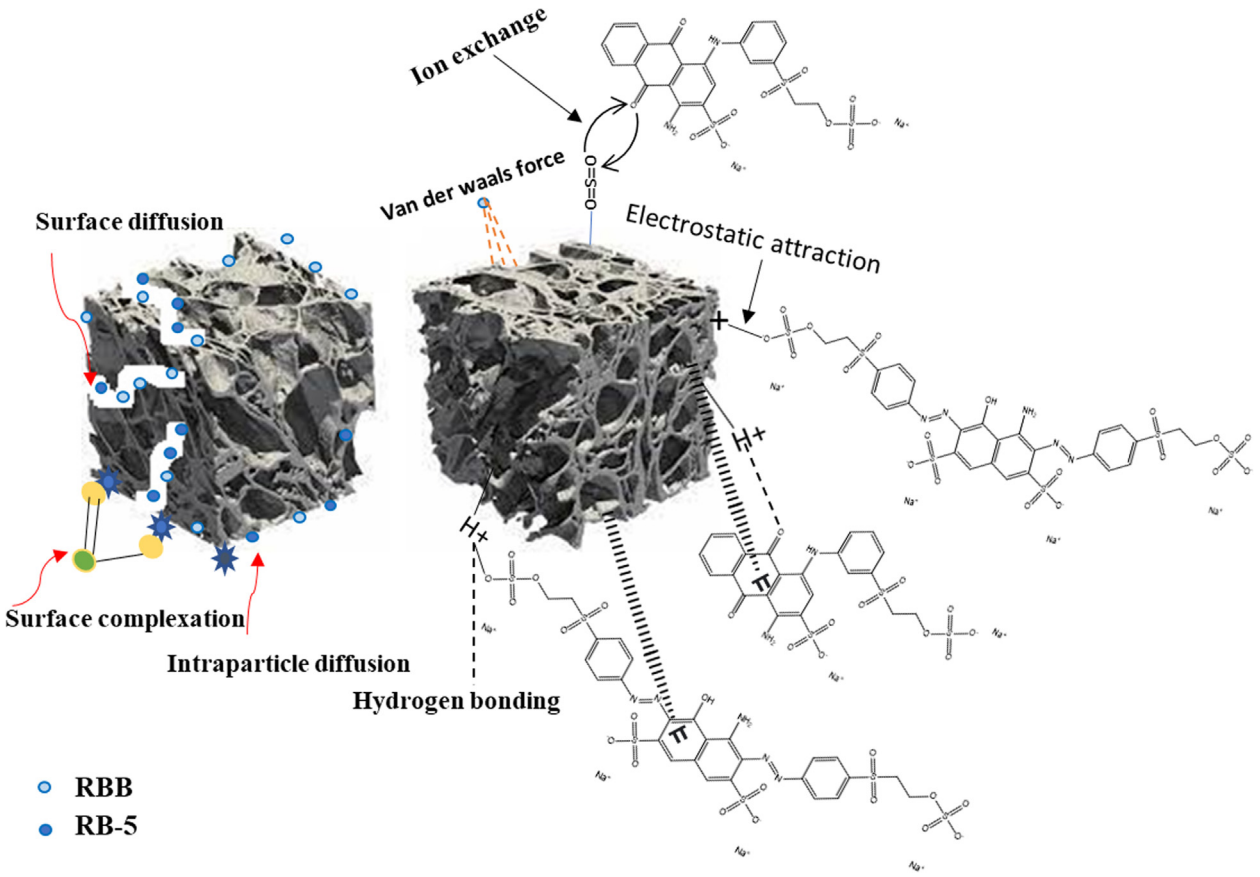


**Fig. 11** Removal mechanism of RBB and RB-5 by DRHB.

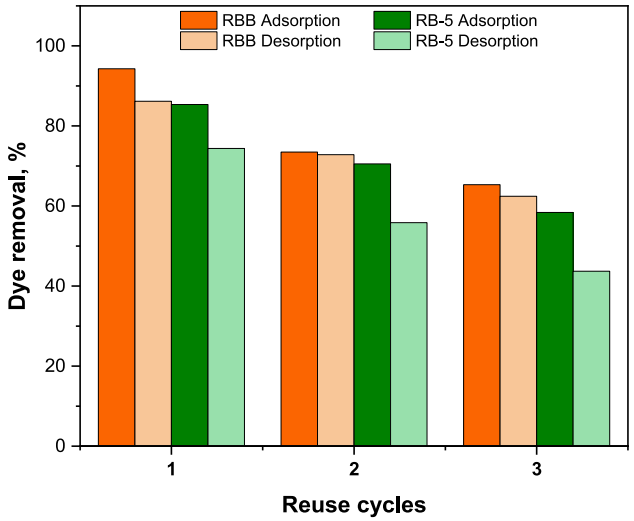


**Fig. 12** Adsorption-Desorption cycle of DRHB using NaOH as desorbing agent.

on biochar surface which could cause the decrease in the adsorption due to the saturation of dyes molecules on DRHB surface and restricting the availability of active sites for further adsorption.

A similar desorption study on RB-5 using gasification residue biochar was conducted by do Nascimento et al. (do Nascimento et al., 2021). After three rounds of adsorption and desorption, regenerated biochar still effectively absorbs the RB-5, after which the removal percentage declined by 50%. Ak, P. et al. (Ak et al., 2020) used acidic and basic eluents for the desorption study and found NaOH as a best medium using which the biochar showed 99.2% desorption efficiency after three cycles. The high adsorption potential of DRHB for both dyes even after three desorption cycles indicates its excellent economic value.

## 4. Conclusion

The dolomite modified biochar (DRHB) was successfully fabricated after ultrasonic pretreatment of rice husk biomass with dolomite (a cheap modifier), following pyrolysis. The adsorption of both dyes on DRHB was facilitated by electrostatic attraction and π-π bonding. Chemisorption is shown as the primary adsorption process in the kinetics investigation of both biochars, as both biochar followed pseudo-second order model. The DRHB exhibited high adsorption capacity for RBB and RB-5 with Langmuir $q_{max}$ of 52.07 and 35.52 mg/g, respectively. The economical recycling property of DRHB was shown by the fact that even after three adsorption–desorption cycles using NaOH, the adsorption% of DRHB for RBB and RB-5 was 65.31 and 58.39%, respectively. The isothermal data of both dyes was well fitted to Langmuir isotherm than Freundlich isotherm, suggesting monolayer adsorption. The cost analysis studies can be done to evaluate the production cost of adsorbent. The spent biochar could be used as a fertilizer after desorbing the dyes. More research is required to determine how to properly dispose of used biochar. Alternative modification methods, such as post-modification of biochar

with dolomite, may be used to evaluate their impact on the characteristics and adsorption capacity of biochar. Future research might explore the effects of various natural minerals on the elimination of emerging organic contaminants and the capacity of the material to be used in broad remediation operations.

## Declaration of Competing Interest

The authors declare that they have no known competing financial interests or personal relationships that could have appeared to influence the work reported in this paper.

## Acknowledgements

This publication is based upon work supported by the National Institute of Food and Agriculture, U.S. Department of Agriculture, McIntire Stennis project under accession number 70011735. This manuscript is publication #SB1102 of the Sustainable Bioproducts, Mississippi State University.

## References

Ahmed, A., Majewska-Nowak, K., Grzegorzek, M., 2021. Removal of reactive dyes from aqueous solutions using ultrafiltration membranes. Environ. Protect. Eng. 47. https://doi.org/10.37190/epe210309.

Ak, P., Ravindiran, G., Vijayakumar, A., et al, 2020. Biodecolorization of Remazol dyes using biochar derived from Ulva reticulata: isotherm, kinetics, desorption, and thermodynamic studies. Desal. water treat. 200, 286–295 http://dx.doi.org/10.5004/dwt.2020.26098.

Al Kausor, M., Sen Gupta, S., Bhattacharyya, K.G., et al, 2022. Montmorillonite and modified montmorillonite as adsorbents for removal of water soluble organic dyes: A review on current status of the art. Inorg. Chem. Commun. 143,. https://doi.org/10.1016/j.inoche.2022.109686 109686.

Amen, R., Bashir, H., Bibi, I., et al, 2020. A critical review on arsenic removal from water using biochar-based sorbents: The significance of modification and redox reactions. Chem. Eng. J. 396,. https://doi.org/10.1016/j.cej.2020.125195 125195.

Aracagök, Y.D., 2022. Biosorption of Remazol Brilliant Blue R dye onto chemically modified and unmodified Yarrowia lipolytica biomass. Arch. Microbiol. 204, 128. https://doi.org/10.1007/s00203-021-02743-3.

Ardila-Leal, L.D., Poutou-Piñales, R.A., Pedroza-Rodríguez, A.M., et al, 2021. A brief history of colour, the environmental impact of synthetic dyes and removal by using laccases. Molecules 26, 3813. https://doi.org/10.3390/molecules26133813.

Arya, M.C., Bafila, P.S., Mishra, D., et al, 2020. Adsorptive removal of Remazol Brilliant Blue R dye from its aqueous solution by activated charcoal of Thuja orientalis leaves: an eco-friendly approach. SN Appl. Sci. 2, 265. https://doi.org/10.1007/s42452-020-2063-2.

Bedin, K.C., de Azevedo, S.P., Leandro, P.K.T., et al, 2017. Bone char prepared by CO2 atmosphere: Preparation optimization and adsorption studies of Remazol Brilliant Blue R. J. Clean. Prod. 161, 288–298. https://doi.org/10.1016/j.jclepro.2017.05.093.

Ben Ayed, A., Hadrich, B., Sciara, G., et al, 2022. Optimization of the decolorization of the Reactive Black 5 by a laccase-like active cell-free supernatant from Coriolopsis gallica. Microorganisms 10, 1137.

Bombuwala Dewage, N., Liyanage, A.S., Smith, Q., et al, 2019. Fast aniline and nitrobenzene remediation from water on magnetized and nonmagnetized Douglas fir biochar. Chemosphere 225, 943–953. https://doi.org/10.1016/j.chemosphere.2019.03.050.

Cardoso, N.F., Lima, E.C., Pinto, I.S., et al, 2011. Application of cupuassu shell as biosorbent for the removal of textile dyes from aqueous solution. J. Environ. Manage. 92, 1237–1247. https://doi.org/10.1016/j.jenvman.2010.12.010.

Chang, M., Shih, Y.-H., 2018. Synthesis and application of magnetic iron oxide nanoparticles on the removal of Reactive Black 5: Reaction mechanism, temperature and pH effects. J. Environ. Manage. 224, 235–242. https://doi.org/10.1016/j.jenvman.2018.07.021.

Cheng, N., Wang, B., Wu, P., et al, 2021. Adsorption of emerging contaminants from water and wastewater by modified biochar: A review. Environ. Pollut. 273,. https://doi.org/10.1016/j.envpol.2021.116448 116448.

do Nascimento, de Araujo, C.M.B., do Nascimento, A.C., et al, 2021. Adsorption of Reactive Black 5 and Basic Blue 12 using biochar from gasification residues: Batch tests and fixed-bed breakthrough predictions for wastewater treatment. Biores. Technol. Rep. 15, 100767. https://doi.org/10.1016/j.biteb.2021.100767.

Dutta, S., Gupta, B., Srivastava, S.K., et al, 2021. Recent advances on the removal of dyes from wastewater using various adsorbents: a critical review. Mat. Adv. 2, 4497–4531. https://doi.org/10.1039/D1MA00354B.

Elsayed, I., Madduri, S., El-Giar, E.M., et al, 2022. Effective removal of anionic dyes from aqueous solutions by novel polyethyleniminе-ozone oxidized hydrochar (PEI-OzHC) adsorbent. Arab. J. Chem. 15,. https://doi.org/10.1016/j.arabjc.2022.103757 103757.

Eltaweil, A.S., Ali Mohamed, H., Abd El-Monaem, E.M., et al, 2020. Mesoporous magnetic biochar composite for enhanced adsorption of malachite green dye: Characterization, adsorption kinetics, thermodynamics and isotherms. Adv. Powder Technol. 31, 1253–1263. https://doi.org/10.1016/j.apt.2020.01.005.

Eltaweil, A.S., Abdelfatah, A.M., Hosny, M., et al, 2022. Novel biogenic synthesis of a Ag@Biochar nanocomposite as an antimicrobial agent and photocatalyst for Methylene Blue degradation. ACS Omega. 7, 8046–8059. https://doi.org/10.1021/acsomega.1c07209.

Elwakeel, K.Z., 2009. Removal of Reactive Black 5 from aqueous solutions using magnetic chitosan resins. J. Hazard. Mater. 167, 383–392. https://doi.org/10.1016/j.jhazmat.2009.01.051.

Eren, Z., Acar, F.N., 2007. Equilibrium and kinetic mechanism for Reactive Black 5 sorption onto high lime Soma fly ash. J. Hazard. Mater. 143, 226–232. https://doi.org/10.1016/j.jhazmat.2006.09.017.

Fang, C., Zhang, T., Li, P., et al, 2015. Phosphorus recovery from biogas fermentation liquid by Ca–Mg loaded biochar. J. Environ. Sci. 29, 106–114. https://doi.org/10.1016/j.jes.2014.08.019.

Feng, L., Liu, J., Guo, Z., et al, 2022. Reactive black 5 dyeing wastewater treatment by electrolysis-Ce (IV) electrochemical oxidation technology: Influencing factors, synergy and enhancement mechanisms. Sep. Purif. Technol. 285,. https://doi.org/10.1016/j.seppur.2021.120314 120314.

Gokulan, R., Prabhu, G.G., Jegan, J., 2019. Remediation of complex remazol effluent using biochar derived from green seaweed biomass. Int. J. Phytoremed. 21, 1179–1189. https://doi.org/10.1080/15226514.2019.1612845.

Hassan, M.M., Carr, C.M., 2018. A critical review on recent advancements of the removal of reactive dyes from dyehouse effluent by ion-exchange adsorbents. Chemosphere 209, 201–219. https://doi.org/10.1016/j.chemosphere.2018.06.043.

He, X., Yang, D.-P., Zhang, X., et al, 2019. Waste eggshell membrane-templated CuO-ZnO nanocomposites with enhanced adsorption, catalysis and antibacterial properties for water purification. Chem. Eng. J. 369, 621–633. https://doi.org/10.1016/j.cej.2019.03.047.

Hii, H.T., 2021. Adsorption isotherm and kinetic models for removal of Methyl Orange and remazol Brilliant Blue R by coconut shell activated carbon. Aquat. Soil Poll. 1, 1–10. https://doi.org/10.53623/tasp.v1i1.4.

Huang, Y., Zeng, X., Guo, L., et al, 2018. Heavy metal ion removal of wastewater by zeolite-imidazolate frameworks. Sep. Purif. Technol. 194, 462–469.

Ihsanullah, I., Jamal, A., Ilyas, M., et al, 2020. Bioremediation of dyes: Current status and prospects. J. Water Process. Eng. 38,. https://doi.org/10.1016/j.jwpe.2020.101680 101680.

Islam, A., Teo, S.H., Taufiq-Yap, Y.H., et al, 2021. Step towards the sustainable toxic dyes removal and recycling from aqueous solution- A comprehensive review. Resour. Conserv. Recycl. 175,. https://doi.org/10.1016/j.resconrec.2021.105849 105849.

Kamali, M., Appels, L., Kwon, E.E., et al, 2021. Biochar in water and wastewater treatment - a sustainability assessment. Chem. Eng. J. 420,. https://doi.org/10.1016/j.cej.2021.129946 129946.

Kapoor, R. T., Rafatullah, M., Siddiqui, M.R., et al, 2022. Removal of Reactive Black 5 Dye by Banana Peel Biochar and Evaluation of Its Phytotoxicity on Tomato. Sustainability 14, 7 https://doi.org/10.3390/su14074176.

Lai, H.J., 2021. Adsorption of remazol Brilliant Violet 5R (RBV-5R) and remazol Brilliant Blue R (RBBR) from aqueous solution by using agriculture waste. Trop. Aqua. Soil Poll. 1, 11–23. https://doi.org/10.53623/tasp.v1i1.10.

Langmuir, I., 1918. The adsorption of gases on plane surfaces of glass, mica and platinum. J. Am. Chem. Soc. 40, 1361–1403. https://doi.org/10.1021/ja02242a004.

Li, J., Li, B., Huang, H., et al, 2019. Removal of phosphate from aqueous solution by dolomite-modified biochar derived from urban dewatered sewage sludge. Sci. Total Environ. 687, 460–469. https://doi.org/10.1016/j.scitotenv.2019.05.400.

Li, Z., Zhang, J., Qu, C., et al, 2021. Synthesis of Mg-Al hydrotalcite clay with high adsorption capacity. Materials 14, 7231. https://doi.org/10.3390/ma14237231.

Madduri, S., Elsayed, I., Hassan, E.B., 2020. Novel oxone treated hydrochar for the removal of Pb(II) and methylene blue (MB) dye from aqueous solutions. Chemosphere 260,. https://doi.org/10.1016/j.chemosphere.2020.127683 127683.

Mahmoud, A.S., Ghaly, A.E., Brooks, S.L., 2007. Influence of Temperature and pH on the Stability and Colorimetric Measurement of Textile Dyes. American Journal of Biochemistry and Biotechnology 3. https://doi.org/10.3844/ajbbsp.2007.33.41.

Mahmoud, A., Ghaly, A., Brooks, S., 2007. Influence of temperature and pH on the stability and colorimetric measurement of textile dyes. Am. J. Biochem. Biotechnol. 3, 33–41. https://doi.org/10.3844/ajbbsp.2007.33.41.

Mate, C.J., Mishra, S., 2020. Synthesis of borax cross-linked Jhingan gum hydrogel for remediation of Remazol Brilliant Blue R (RBBR) dye from water: Adsorption isotherm, kinetic, thermodynamic and biodegradation studies. Int. J. Biol. Macromol. 151, 677–690. https://doi.org/10.1016/j.ijbiomac.2020.02.192.

Mecozzi, M., Pietroletti, M., Scarpiniti, M., et al, 2012. Monitoring of marine mucilage formation in Italian seas investigated by infrared spectroscopy and independent component analysis. Environ. Monit. Assess. 184, 6025–6036. https://doi.org/10.1007/s10661-011-2400-4.

Mittal, J., 2021. Recent progress in the synthesis of Layered Double Hydroxides and their application for the adsorptive removal of dyes: A review. J. Environ. Manage. 295,. https://doi.org/10.1016/j.jenvman.2021.113017 113017.

Munagapati, V.S., Yarramuthi, V., Kim, Y., et al, 2018. Removal of anionic dyes (Reactive Black 5 and Congo Red) from aqueous solutions using Banana Peel Powder as an adsorbent. Ecotoxicol. Environ. Saf. 148, 601–607. https://doi.org/10.1016/j.ecoenv.2017.10.075.

Munagapati, V.S., Wen, J.-C., Pan, C.-L., et al, 2020. Adsorptive removal of anionic dye (Reactive Black 5) from aqueous solution using chemically modified banana peel powder: kinetic, isotherm, thermodynamic, and reusability studies. Int. J. Phytoremed. 22, 267–278. https://doi.org/10.1080/15226514.2019.1658709.

Murugesan, A., Loganathan, M., Senthil Kumar, P., et al, 2021. Cobalt and nickel oxides supported activated carbon as an effective photocatalysts for the degradation Methylene Blue dye from aquatic environment. Sustain. Chem. Pharm. 21,. https://doi.org/10.1016/j.scp.2021.100406 100406.

Nagendrappa, G., 2004. An epitome of K Venkataraman's chemistry. Resonance 9, 45–51. https://doi.org/10.1007/BF02834306.

Namasivayam, E., Manimaran, D., Sulthana, A., 2018. Reactive black 5 induced developmental defects via potentiating apoptotic cell death in Zebrafish (Danio rerio) embryos. Pharm. Pharmacol. Int. J. 6, 449–451. https://doi.org/10.15406/ppij.2018.06.00216.

Nandanwar, P.M., Saravanan, D., Bakshe, P., et al, 2022. Chitosan entrapped microporous activated carbon composite as a supersorbent for remazol brilliant blue R. Mat. Adv. 3, 5488–5496. https://doi.org/10.1039/D2MA00508E.

Nguyen, D.L.T., Binh, Q.A., Nguyen, X.C., et al, 2021. Metal salt-modified biochars derived from agro-waste for effective congo red dye removal. Environ. Res. 200,. https://doi.org/10.1016/j.envres.2021.111492 111492.

Nguyen, T.T., Chen, H.-H., To, T.H., et al, 2021. Development of biochars derived from water bamboo (Zizania latifolia) shoot husks using pyrolysis and ultrasound-assisted pyrolysis for the treatment of Reactive Black 5 (RB5) in wastewater. Water 13, 1615. https://doi.org/10.3390/w13121615.

Nidheesh, P.V., Zhou, M., Oturan, M.A., 2018. An overview on the removal of synthetic dyes from water by electrochemical advanced oxidation processes. Chemosphere 197, 210–227. https://doi.org/10.1016/j.chemosphere.2017.12.195.

Parimelazhagan, V., Yashwath, P., Arukkani Pushparajan, D., et al, 2022. Rapid removal of toxic Remazol Brilliant Blue-R dye from aqueous solutions using Juglans nigra shell biomass activated carbon as potential adsorbent: Optimization, isotherm, kinetic, and thermodynamic investigation. Int. J. Mol. Sci. 23, 12484. https://doi.org/10.3390/ijms232012484.

Qiu, B., Tao, X., Wang, H., et al, 2021. Biochar as a low-cost adsorbent for aqueous heavy metal removal: A review. J. Anal. Appl. Pyrolysis 155,. https://doi.org/10.1016/j.jaap.2021.105081 105081.

Rahmat, N. A., Ali, A. A., Salmiati, et al, 2016. Removal of Remazol Brilliant Blue R from Aqueous Solution by Adsorption Using Pineapple Leaf Powder and Lime Peel Powder. Water, Air Soil Poll 227, 105. https://link.springer.com/article/10.1007/s11270-016-2807-0031.

Raj, A., Yadav, A., Rawat, A.P., et al, 2021. Kinetic and thermodynamic investigations of sewage sludge biochar in removal of Remazol Brilliant Blue R dye from aqueous solution and evaluation of residual dyes cytotoxicity. Environ. Technol. Innov. 23,. https://doi.org/10.1016/j.eti.2021.101556 101556.

Reghioua, A., Barkat, D., Jawad, A.H., et al, 2021. Magnetic chitosan-glutaraldehyde/zinc oxide/Fe3O4 nanocomposite: Optimization and adsorptive mechanism of Remazol Brilliant Blue R dye removal. J. Polym. Environ. 29, 3932–3947. https://doi.org/10.1007/s10924-021-02160-z.

Ren, J., Li, N., Li, L., et al, 2015. Granulation and ferric oxides loading enable biochar derived from cotton stalk to remove phosphate from water. Biores. Technol. 178, 119–125. https://doi.org/10.1016/j.biortech.2014.09.071.

Renita, A.A., Vardhan, K.H., Kumar, P.S., et al, 2021. Effective removal of malachite green dye from aqueous solution in hybrid system utilizing agricultural waste as particle electrodes. Chemosphere 273,. https://doi.org/10.1016/j.chemosphere.2021.129634 129634.

Sahoo, T.R., Prelot, B., 2020. Chapter 7 - Adsorption processes for the removal of contaminants from wastewater: the perspective role of nanomaterials and nanotechnology. In: Bonelli, B., Freyria, F.S., Rossetti, I. (Eds.), Nanomaterials for the Detection and Removal of Wastewater Pollutants. Elsevier, pp. 161–222.

Salleh, M.A.M., Mahmoud, D.K., Karim, W.A.W.A., et al, 2011. Cationic and anionic dye adsorption by agricultural solid wastes: A comprehensive review. Desalination 280, 1–13. https://doi.org/10.1016/j.desal.2011.07.019.

Silva, T.L., Ronix, A., Pezoti, O., et al, 2016. Mesoporous activated carbon from industrial laundry sewage sludge: Adsorption studies of reactive dye Remazol Brilliant Blue R. Chem. Eng. J. 303, 467–476. https://doi.org/10.1016/j.cej.2016.06.009.

Singh, M., Ahsan, M., Pandey, V., et al, 2022. Comparative assessment for removal of anionic dye from water by different waste-derived biochar vis a vis reusability of generated sludge. Biochar 4, 13. https://doi.org/10.1007/s42773-022-00140-7.

Sonal, S., Singh, A., Mishra, B.K., 2018. Decolorization of reactive dye Remazol Brilliant Blue R by zirconium oxychloride as a novel coagulant: optimization through response surface methodology. Water Sci. Technol. 78, 379–389. https://doi.org/10.2166/wst.2018.307.

Srivastava, A., Rani, R.M., Patle, D.S., et al, 2022. Emerging bioremediation technologies for the treatment of textile wastewater containing synthetic dyes: a comprehensive review. J. Chem. Technol. & Biotechnol. 97, 26–41. https://doi.org/10.1002/jctb.6891.

Srivastava, A., Dangi, L.K., Kumar, S., et al, 2022. Microbial decolorization of Reactive Black 5 dye by Bacillus albus DD1 isolated from textile water effluent: kinetic, thermodynamics & decolorization mechanism. Heliyon 8. https://doi.org/10.1016/j.heliyon.2022.e08834 e08834.

Steigerwald, J.M., Ray, J.R., 2021. Adsorption behavior of perfluorooctanesulfonate (PFOS) onto activated spent coffee grounds biochar in synthetic wastewater effluent. J. Hazard. Mat. Lett. 2,. https://doi.org/10.1016/j.hazl.2021.100025 100025.

Uddin, M.J., Ampiaw, R.E., Lee, W., 2021. Adsorptive removal of dyes from wastewater using a metal-organic framework: A review. Chemosphere 284,. https://doi.org/10.1016/j.chemosphere.2021.131314 131314.

Wanyonyi, W.C., Mulaa, F.J., 2020. Alkaliphilic Enzymes and Their Application in Novel Leather Processing Technology for Next-Generation Tanneries. In: Mamo, G., Mattiasson, B. (Eds.), Alkaliphiles in Biotechnology. Publishing, Cham, Springer International, pp. 195–220.

Xu, H., Boeuf, G., Jia, Z., et al, 2021. Solvent-free synthesized monolithic ultraporous aluminas for highly efficient removal of Remazol Brilliant Blue R: Equilibrium, kinetic, and thermodynamic studies. Materials 14, 3054. https://doi.org/10.3390/ma14113054.

Xu, K., Lin, F., Dou, X., et al, 2018. Recovery of ammonium and phosphate from urine as value-added fertilizer using wood waste biochar loaded with magnesium oxides. Clean. Prod. 187, 205–214. https://doi.org/10.1016/j.jclepro.2018.03.206.

Yuan, J.-H., Xu, R.-K., Zhang, H., 2011. The forms of alkalis in the biochar produced from crop residues at different temperatures. Biores. Technol. 102, 3488–3497. https://doi.org/10.1016/j.biortech.2010.11.018.

Zhang, X.N., Mao, G.Y., Jiao, Y.B., et al, 2014. Adsorption of anionic dye on magnesium hydroxide-coated pyrolytic bio-char and reuse by microwave irradiation. Int. J. Environ. Sci. Technol. 11, 1439–1448. https://doi.org/10.1007/s13762-013-0338-5.

Zhang, H., Xing, L., Liang, H., et al, 2022. Efficient removal of Remazol Brilliant Blue R from water by a cellulose-based activated carbon. Int. J. Biol. macromol. 207, 254–262. https://doi.org/10.1016/j.ijbiomac.2022.02.174.